Journal of Zhejiang University-SCIENCE B (Biomedicine & Biotechnology)
ISSN 1673-1581 (Print); ISSN 1862-1783 (Online)
www.jzus.zju.edu.cn; www.springerlink.com
E-mail: jzus@zju.edu.cn

Preliminary study on the role of novel LysR family gene *kp05372* in *Klebsiella pneumoniae* of forest musk deer*

Wei YANG[§1], Wu-you WANG[§1], Wei ZHAO[1], Jian-guo CHENG[2], Yin WANG[1], Xue-ping YAO[1], Ze-xiao YANG[1], Dong YU[1], Yan LUO[†‡1]

[1]*College of Veterinary Medicine, Sichuan Agricultural University, Wenjiang 611130, China*

[2]*Sichuan Institute of Musk Deer Breeding, Dujiangyan 611830, China*

[†]E-mail: lycjg@163.com

Received June 22, 2019; Revision accepted Sept. 25, 2019; Crosschecked Dec. 25, 2019; Published online Feb. 5, 2020

Abstract: LysR-type transcriptional regulators are involved in the regulation of numerous cellular metabolic processes in *Klebsiella pneumoniae*, leading to severe infection. Earlier, we found a novel LysR family gene, named *kp05372*, in a strain of *K. pneumoniae* (designated GPKP) isolated from forest musk deer. To study the function of this gene in relation to the biological characteristics of GPKP, we used the suicide plasmid and conjugative transfer methods to construct deletion mutant strain GPKP-Δ*kp05372*; moreover, we also constructed the GPKP-Δ*kp05372*$^{+}$ complemented strain. The role of this gene was determined by comparing the following characteristics of three strains: growth curves, biofilm formation, drug resistance, stress resistance, median lethal dose (LD_{50}), organ colonization ability, and the histopathology of GPKP. Real-time polymerase chain reaction (RT-PCR) was used to test the expression level of seven genes upstream of *kp05372*. There was no significant difference in the growth rates when comparing the three bacterial strains, and no significant difference was recorded at different osmotic pressures, temperatures, salt contents, or hydrogen peroxide concentrations. The GPKP-Δ*kp05372* mutant formed a weak biofilm, and the other two strains formed medium biofilm. The drug resistance of the GPKP-Δ*kp05372* mutant toward cephalothin, cotrimoxazole, and polymyxin B was changed. The acid tolerance of the deletion strain was stronger than that of the other two strains. The LD_{50} values of the wild-type and complemented strains were 174-fold and 77-fold higher than that of the GPKP-Δ*kp05372* mutant, respectively. The colonization ability of the GPKP-Δ*kp05372* mutant in the heart, liver, spleen, kidney, and intestine was the weakest. The three strains caused different histopathological changes in the liver and lungs. In the GPKP-Δ*kp05372* mutant, the relative expression levels of *kp05374* and *kp05379* were increased to 1.32-fold and 1.42-fold, respectively, while the level of *kp05378* was decreased by 42%. Overall, the deletion of *kp05372* gene leads to changes in the following: drug resistance and acid tolerance; decreases in virulence, biofilm formation, and colonization ability of GPKP; and regulation of the upstream region of adjacent genes.

Key words: *Moschus berezovskii*; *Klebsiella pneumoniae*; LysR transcription factor; *kp05372* gene; Biological characteristics; Upstream gene

https://doi.org/10.1631/jzus.B1900440 **CLC number:** S858.94; Q78

1 Introduction

Klebsiella pneumoniae has been regarded as an opportunistic pathogen in animal respiratory and intestinal tracts and is currently recognized as a Gram-negative bacterium that causes human and animal diseases. It can lead to human and animal enteritis, pneumonia, liver abscess, peritonitis, bronchitis and

‡ Corresponding author
§ The two authors contributed equally to this work
* Project supported by the Sichuan Province Academic and Technical Leadership Development Funding Project and the Science & Technology Achievements Transfer Project of Sichuan (No. 2017YSZH0008), China
ORCID: Yan LUO, https://orcid.org/0000-0001-8156-6572

wound infection, as well as meningitis, septicemia, and gastrointestinal diseases, which pose great difficulties in clinical treatment, with extremely high morbidity and mortality (Bujanda et al., 1996; O'Toole et al., 2000; Roberts et al., 2000; Fang et al., 2004; Lederman and Crum, 2005). The forest musk deer (*Moschus berezovskii*), a rare economic animal, is seriously restricted by pneumonia, which has a serious impact on its breeding. *K. pneumoniae* is one of the pathogenic organisms that cause pneumonia in musk deer, and most of them colonize on the mucosal surface of mammals, with a high clinical infection rate, which can lead to pneumonia and even death in musk deer (Yang et al., 2017). Pneumonia in musk deer is characterized by dyspnea, pulmonary hemorrhage, and purulent lesions in the lungs and other parenchymal organs. *K. pneumoniae* is difficult to be controlled effectively in captive forest musk deer.

In our previous study, a strain of *K. pneumoniae* (designated GPKP) was isolated from the feces of forest musk deer that were bred at the Baisha Musk Deer Farm in Sichuan Institute of Musk Deer Breeding (Dujiangyan, China) and were suffering from purulent pneumonia and diarrhea (Zhao et al., 2017b). A novel LysR family gene, named *kp05372*, had been identified by whole-genome sequencing of GPKP. The related physicochemical properties and the structural prediction of the coding product of gene *kp05372* indicated that the *kp05372*-encoded protein is a typical LysR transcription factor. Research into the LysR-type transcriptional regulator (LTTR) family began in the 1980s and first appeared in reports published by Henikoff et al. (1988). It is the largest family of prokaryotic transcriptional binding proteins and can regulate the expression of genes with different functions, including some important functions during the interaction between prokaryotes and eukaryotes. Proteins of this family have a unique structure, with an N-terminal DNA-binding helix-turn-helix motif and a C-terminal coinducer-binding domain (Maddocks and Oyston, 2008). The LysR family genes have similar characteristics, often adjacent to and opposite to their target genes, and their promoter regions overlap with each other for the purpose of regulating expression (Viswanathan et al., 2007).

Analysis of the adjacent genes of *kp05372* found that the upstream seven adjacent genes had their transcription direction opposite to that of *kp05372*. We named them *kp05373*, *kp05374*, *kp05375*, *kp05376*, *kp05377*, *kp05378*, and *kp05379* in their respective order. The interval between *kp05372* and *kp05373* is 475-bp long. Through promoter prediction analysis, the DNA sequence of the interval between the two genes has been found to have obvious positive and negative promoter characteristics, and the promoter regions also overlap. Therefore, they may have regulatory relationships, which is the typical feature of the LysR family of transcriptional regulators. LTTRs have a wide range of regulatory functions in bacteria. The target genes of regulation are involved in bacterial cell division, virulence, metabolism, quorum sensing, motility, antioxidant reaction, nitrogen fixation, adhesion, and secretion (Frisch and Bender, 2010; Lee et al., 2013; Srinivasan et al., 2013). Consequently, we think that it may also be functionally similar to other genes in the LysR family and may be involved in regulating the virulence, catabolism, drug resistance, and host colonization ability of *K. pneumoniae* in forest musk deer, and that it may also regulate the expression of its adjacent genes to regulate the physiological functions determined by its adjacent genes.

In this study, to explore the basic function of the newly discovered LTTR gene *kp05372*, the mutant and the complemented strains of GPKP were constructed, the differences in biological characteristics, such as growth curve, drug sensitivity, biofilm formation, stress resistance, median lethal dose (LD_{50}), colonization ability, and histopathological morphology, between the two strains and the wild-type strain were compared, and the expression levels of seven genes upstream of *kp05372* in the mutant were determined.

2 Materials and methods

2.1 Bacterial strains, plasmids, and media

K. pneumoniae of musk deer GPKP (GenBank: KX929840.1) was provided by the Animal Quarantine Laboratory, Wenjiang Campus, Sichuan Agricultural University (Chengdu, China). *Escherichia coli* DH5α and the pMD-19T plasmid were purchased from TaKaRa Biomedical Technology (Beijing) Co., Ltd. Suicide vector pLP12T, expression plasmid pBAD33, and *E. coli* β2163 were obtained from

Guangzhou KnoGen Biotech Co., Ltd. Luria-Bertani (LB) broth, Mueller-Hinton (MH) medium, and MacConkey media were purchased from Chengdu Haoboyou Technology Co., Ltd.

2.2 Primer design

The primer pair KP-M1F/KP-M1R was amplified to obtain the fragment A of the upstream homologous arm of *kp05372*. The primer KP-M1F was composed of two parts, the 5'-end lowercase letters indicating the homologous sequence of the suicide vector pLP12T and the 3'-end being the homologous sequence of the upstream homologous arm of the gene to be knocked out. The primer pair KP-M2F/KP-M2R was amplified to obtain the downstream homologous arm fragment B of *kp05372*. The primer KP-M2R was composed of two parts, the 5'-end lowercase letters denoting the homologous sequence of the suicide vector pLP12T, and the 3'-end being the homologous sequence of the downstream homologous arm of the gene to be knocked out. The underlined part of the 5'-end of the primer KP-M1R was the complementary reverse sequence of the downstream homologous arm B amplification primer KP-M2F of the gene to be knocked out. The bold part of the 5'-end primer KP-M2F is the complementary reverse sequence of the upstream homologous arm A amplification primer of the gene. The primer pair KP-PF/KP-PR was used to identify the mutant. The primer pair pLP-UF/pLP-UR was used to identify the recombinant suicide plasmid. The primer pair pBAD33-ZF/pBAD33-ZR was used as the vector amplification primer. The primer pair KP-RF/KP-RR was used as the primers for the gene to be knocked out. The primer pair pBAD33-mcf-TF/pBAD33-mcf-TR was used to identify the complemented strain. The primer pairs of *kp05373*, *kp05374*, *kp05375*, *kp05376*, *kp05377*, *kp05378*, *kp05379*, and *recA* were used for real-time polymerase chain reaction (RT-PCR) to determine the regulatory effect of *kp05372* on seven upstream genes. The specific primer sequences are shown in Table 1.

2.3 DNA extraction and purification

According to the manufacturer's instructions, total genomic DNA was extracted from samples of the bacterial solutions using the Bacterial Genome DNA Extraction Kit (Tiangen Biotech, China) and stored at −20 °C. The quantity and quality of the extracted DNAs were measured using a NanoDrop 2000 spectrophotometer (Thermo Fisher Scientific, USA) and agarose gel electrophoresis, respectively.

2.4 DNA manipulation and construction of the GPKP-Δ*kp05372* mutant

The upstream homologous arm A and the downstream homologous arm B of the *kp05372* gene were amplified by PCR using the genome of GPKP as template and using primer pairs KP-M1F/KP-M1R and KP-M2F/KP-M2R, respectively. Homologous arms A and B were purified using the PCR Product Purification Kit (Tiangen). The purified homologous arms A and B were used as the template, and KP-M1F and KP-M2R were used as primers for overlap extension PCR amplification to obtain the fused fragment AB. Using the ClonExpress II One Step Cloning Kit (Vazyme, China), the fused fragment AB was cloned seamlessly with the suicide vector pLP12T to construct the recombinant suicide plasmid pLP12T-*kp05372*. The pLP12T-*kp05372* plasmid was transformed into *E. coli* β2163, and the primer pair pLP-UF/pLP-UR was used to screen for positive clones. After the coculture of 1.5 mL positive clones and 0.5 mL GPKP to enable conjugative transfer, 100 μL samples of the mixture were plated onto LB solid medium with 20 μg/mL chloramphenicol (CM), and the zygotes were screened by PCR using the primer pair KP-M1F/KP-M2R. Zygotes were spread onto LB solid medium with 0.4% L-arabinose and cultured overnight at 30 °C, with screening by analytical PCR using the primer pair KP-PF/KP-PR. After the zygotes were purified, the DNA was amplified again, and sequencing of the PCR product was used to verify the successful construction of the deletion strain GPKP-Δ*kp05372* mutant.

2.5 Construction of the GPKP-Δ*kp05372*$^+$ complemented strain

We used the genome of GPKP as the template and KP-RF/KP-RR as the primer pair to perform PCR to obtain the expression fragment *kp05372*. Furthermore, we used plasmid pBAD33 as the template and pBAD33-ZF/pBAD33-ZR as the primer pair to perform PCR to obtain the pBAD33 vector fragment.

Table 1 Primer sequences for gene knockout and real-time PCR

Primer	Primer sequence (5'→3')*	T_m (°C)	Product length (bp)
KP-M1	F: ggaatctagaccttgagtcgCGTCATCTTCTACAATCGCAGTCTC	56.0	638
	R: TTGTTCACCCCCGTGCTGTG**TTTGAGTCGGTTGAAACTGATCCC**		
KP-M2	F: **GGGATCAGTTTCAACCGACTCAAA**CACAGCACGGGGGTGAACAA	60.0	629
	R: acagctagcgacgatatgtcCATTAGCAGAACCGAGAAACAGGC		
KP-P	F: GCCGATTTTAGGATGTCTGTCACC	58.0	1386/2196
	R: CACCCAGCAGATAGCCCAGCA		
pLP-U	F: GACACAGTTGTAACTGGTCCA	59.0	1517
	R: CAGGAACACTTAACGGCTGAC		
pBAD33-Z	F: CTAGAGTCGACCTGCAGGCA	60.0	5529
	R: AGCTCGAATTCGCTAGCCCA		
KP-R	F: TGGGCTAGCGAATTCGAGCTAGGAGGAATTCACCATGAACGGGATCAGT	58.0	963
	R: TGCCTGCAGGTCGACTCTAGTTAGCTGCGACGCTCCTG		
pBAD33-mcf-T	F: CCATAAGATTAGCGGATCCTACCT	60.0	1067
	R: CTTCTCTCATCCGCCAAAACAG		
kp05373	F: CGGCATTGTTATCGGTGAGA	57.8	174
	R: GAGCCAGCCCCAACGGTA		
kp05374	F: TCCCCAACAACTTTATCG	57.0	126
	R: AAATCCCCTCTTCCCCAC		
kp05375	F: CGGACTCGGTCTTTCTTT	55.8	142
	R: CGCTTTATCTGTTTGGGA		
kp05376	F: GGGGTAAATCCGCCAATA	57.0	112
	R: CGAGAACCTGATACGCAA		
kp05377	F: CACCCCGAGACTGCCTAT	55.8	104
	R: ACCCCCGTTCCTCCTATG		
kp05378	F: TACCACCCGTGACCCCTG	57.7	200
	R: CGTTTTCTGAGCCGACTTTA		
kp05379	F: GCCACACTGCGAAATGAC	55.8	78
	R: CGGCTCCAGATGGTTACA		
recA	F: TTAAACAGGCCGAATTCCAG	61.0	99
	R: CCGCTTTCTCAATCAGCTTC		

T_m: melting temperature. * Lowercase letters indicate the homologous sequence; underlined letters indicate the complementary reverse sequence of the downstream homologous arm B amplification primer of the gene to be knocked out; bold letters indicate the complementary reverse sequence of the upstream homologous arm A amplification primer of the gene

The purified *kp05372* fragment was seamlessly ligated into the pBAD33 vector fragment, and the primer pair pBAD33-mcf-TF/pBAD33-mcf-TR was used for screening for the recombinant clone pBAD33-*kp05372*. The pBAD33-*kp05372* was transformed into *E. coli* β2163, and the transformed products were recovered and cultured for 1 h and coated onto LB plates containing 20 μg/mL CM and 0.3 mmol/L diaminopimelic acid; the clones were screened by PCR using the primer pair pBAD33-mcf-TF/pBAD33-mcf-TR. After coculturing GPKP-Δ*kp05372* mutant and *E. coli* β2163 containing pBAD33-*kp05372* to enable conjugative transfer, the mixture was plated onto LB solid medium (20 μg/mL CM, 0.02%–0.20% L-arabinose) to obtain the recombinant GPKP-Δ*kp05372*$^+$ complemented strain. The recombinant strain was screened by colony PCR using pBAD33-mcf-TF/pBAD33-mcf-TR primer pair and PCR sequencing for validation. Positive clones were purified by streak plating.

2.6 In vitro growth curves

The wild-type GPKP, GPKP-Δ*kp05372* mutant, and GPKP-Δ*kp05372*$^+$ complemented strains stored at −70 °C were plated on LB solid medium and incubated overnight at 37 °C to revive and purify strains. The wild-type GPKP, GPKP-Δ*kp05372* mutant, and GPKP-Δ*kp05372*$^+$ complemented strains were inoculated into 5 mL LB broth and incubated for 6 h at 37 °C. Wild-type GPKP, GPKP-Δ*kp05372* mutant, and GPKP-Δ*kp05372*$^+$ complemented strains were suspended in fresh LB broth to adjust the optical density at 600 nm (OD_{600}) to 0.5. Then, according to the proportion 1:100, each 2 mL aliquot of the bacterial liquid was inoculated into 200 mL LB broth and synchronously incubated for 24 h at 37 °C. Every 2 h, 2 mL were sampled such that 1 mL was used to determine OD_{600} and 1 mL was diluted for colony count. We performed the above test set three times and drew the growth curve.

2.7 RNA isolation and RT-PCR

In this study, the transcriptional levels of the genes upstream of *kp05372*, namely, *kp05373*, *kp05374*, *kp05375*, *kp05376*, *kp05377*, *kp05378*, and *kp05379*, in wild-type GPKP and GPKP-Δ*kp05372* mutant strains, were determined. Total RNA was extracted from the exponential-phase cultures of wild-type GPKP and GPKP-Δ*kp05372* mutant strains using a HiPure Bacterial RNA kit (Magen, China) according to the manufacturer's instructions. The RNA was checked for the absence of DNA contamination and used as template for complementary DNA (cDNA) synthesis using the PrimeScript RT Reagent Kit (TaKaRa). Gene expression levels were monitored by RT-PCR (Bio-Rad, CA, USA), and melting curve analysis was carried out to confirm amplification of a single product. The Pfaffl method (Pfaffl, 2001) was used to compare the relative expression of wild-type GPKP and GPKP-Δ*kp05372* mutant strains. The formula of the Pfaffl method is as follows: ratio=$(1+E_{\text{target}})^{\Delta C_{\text{T}}\text{ target (control−experiment)}}/(1+E_{\text{reference}})^{\Delta C_{\text{T}}\text{ reference (control−experiment)}}$, where E is the amplification efficiency and C_{T} is the number of reaction cycles when the fluorescence signal reaches the detection threshold. The gene amplification efficiency was obtained by establishing the standard curve. The standard substance for establishing the standard curve was obtained by gradient dilution of the plasmid extracted from *E. coli* DH5α containing pMD-19T which was connected to the target gene.

2.8 Biofilm formation assay

The wild-type GPKP, GPKP-Δ*kp05372* mutant, and GPKP-Δ*kp05372*$^{+}$ complemented strains were inoculated in 5 mL LB broth and incubated overnight at 37 °C with shaking at 200 r/min; then, the concentration of bacterial liquid was adjusted to 1×10^{7} CFU/mL (CFU, colony-forming unit). Then, 100 μL medium was added to each well in the 96-well plate, and the bacterial solution was inoculated in a ratio of 1:10. Three replicates were set for each group. After 36 h of incubation at 37 °C, the culture medium was removed, and phosphate-buffered saline (PBS) was used for washing the wells three times to remove free bacteria. Subsequently, 100 μL methanol was added to each well and left undisturbed for 15 min. Then, methanol was removed and the wells were dried naturally. The bound cells were stained for 5 min with 100 μL crystal violet solution (10 g/L) at room temperature. Later, PBS buffer was used for rinsing the wells five times, and 100 μL dimethyl sulphoxide (DMSO) was added after it was completely dried. It was placed on a shaker for 2 h, shaken at an interval of 1 h to dissolve crystal violet, and the OD_{570} value was determined. Medium without inoculation was used as the negative control. The mean OD_{570} value plus the sum of three standard deviations of the negative control was the critical value T (Murphy and Kirkham, 2002).

2.9 Drug sensitivity test

The drug sensitivity tests used the Kirby-Bauer (K-B) agar method as reference (CLSI, 2019). The wild-type GPKP, GPKP-Δ*kp05372* mutant, and GPKP-Δ*kp05372*$^{+}$ complemented strains were inoculated in 50 mL LB broth and incubated for 12 h at 37 °C with shaking at 200 r/min; the bacterial liquid was adjusted to a concentration of 10^{7} CFU/mL, and aliquots (0.2 mL) of the three bacterial solutions were spread onto MH agar medium. Antibiotic disks (Hangzhou Microbial Reagent, China) were put on the surface of the MH agar medium, incubated for 16–18 h at 37 °C, and the diameters of the inhibition zones were measured. The following antimicrobials, including gentamicin (10 μg), tobramycin (10 μg), kanamycin (30 μg), neomycin (30 μg), streptomycin (10 μg), norfloxacin (10 μg), ciprofloxacin (5 μg), enrofloxacin (10 μg), ofloxacin (5 μg), carbenicillin (100 μg), oxacillin (1 μg), piperacillin (100 μg), ampicillin (10 μg), penicillin (10 μg), cefotaxime (30 μg), ceftazidime (30 μg), cefobid (75 μg), cefazolin (30 μg), cefuroxime (30 μg), compound sulfamethoxazole (sulfamethoxazole (23.75 μg)/trimethoprim (1.25 μg)), furazolidone (100 μg), erythromycin (30 μg), chloramphenicol (30 μg), tetracycline (30 μg), polymyxin B (300 IU), vancomycin (30 μg), and augmentin (amoxicillin (20 μg)/clavulanic acid (110 μg)), were tested.

2.10 Stress resistance assay

The wild-type GPKP, GPKP-Δ*kp05372* mutant, and GPKP-Δ*kp05372*$^{+}$ complemented strains were inoculated in 50 mL LB broth and incubated overnight at 37 °C; the bacterial liquid concentration was then adjusted to 1×10^{7} CFU/mL. According to the ratio of 1:50, they were inoculated as follows: into 5 mL LB broth containing 0.1, 0.2, 0.3, 0.4, 0.5, 0.6, 0.7,

and 0.8 mol/L KCl, and LB broth without KCl used as the control; into 5 mL LB broth with pH of 2, 3, 4, 5, 6, 7, 8, 9, and 10, and the medium with pH 7 used as the control (He et al., 2019); into 5 mL LB broth containing 0.1%, 0.5%, 1.0%, 1.5%, 2.0%, 2.5%, 3.0%, 3.5%, and 4.0% NaCl (1%=0.01 g/mL), and the medium containing 1.5% NaCl used as the control; into 5 mL LB broth containing 1, 2, 3, 4, 5, 6, 7, and 8 mmol/L H_2O_2, and medium without H_2O_2 used as the control; and into 5 mL LB broth and incubated for 2 h at 37, 40, 45, 50, 55, and 60 °C, and the sample incubated for 2 h at 37 °C used as the control. After the treatment, the samples were incubated overnight at 37 °C with shaking at 200 r/min, the OD_{600} was measured, and viable cells were counted.

2.11 Infection of SPF KM mice

The 0% lethal dose (LD_0) and absolute lethal dose (LD_{100}) of the wild-type GPKP, GPKP-Δ*kp05372* mutant, and GPKP-Δ*kp05372*$^+$ complemented strains were obtained by screening in the preliminary experiment. A total of 78 SPF KM mice (18–22 g weight, 6 weeks old), half the population being male and half female, were randomly divided into 13 groups with six mice in each group (SPF KM mice were purchased from Chengdu Dashuo Biotechnology Co., Ltd.). The animal experiments were approved by the National Institute of Animal Health Care and Use Committee at Sichuan Agricultural University (approval number SYXK2019-187). During the experiment, all mice were free to eat and to drink water. This experiment was carried out in accordance with the provisions for maintaining an environment of illumination and ventilation, as well as appropriate conditions of feeding and management.

Groups 1–6 were the GPKP-Δ*kp05372* mutant group, Groups 7–12 comprised the GPKP-Δ*kp05372*$^+$ complemented strain group, and Group 13 was the control group. The GPKP-Δ*kp05372* mutant and GPKP-Δ*kp05372*$^+$ complemented strains were inoculated into 5 mL LB broth and incubated overnight at 37 °C with shaking at 200 r/min. According to the results of the preliminary experiments, the concentration of bacterial solution was adjusted as follows: 3.3×10^6 to 3.3×10^{11} CFU/mL in the GPKP-Δ*kp05372* mutant group; and 6.8×10^6 to 6.8×10^{11} CFU/mL in the GPKP-Δ*kp05372*$^+$ complemented strain group. Each group was injected intraperitoneally at a dose of 0.5 mL per mouse for the challenge experiment, while the control group was injected with the same amount of sterilized normal saline. After the challenge experiment, the incidence and mortality of mice in each group were observed for 7 d and recorded in detail. Bliss method was used to calculate LD_{50} (Bliss, 1935).

2.12 Organ colonization assays

A total of 60 SPF KM mice (18–22 g weight, 6 weeks old), half of these being male and half female, were randomly divided into three groups with 20 mice in each group. The bacterial solution was diluted to ten times LD_{50} and inoculated into mice. At 12, 24, 48, 72, and 96 h, the heart, liver, spleen, lung, kidney, and intestine of the mice were collected and weighed. Then, a small amount of tissue was taken, and an appropriate amount of PBS buffer was added to make the mixture of PBS and tissues reach 1 g (Pollak et al., 2015). After grinding, the sample was diluted in multiple proportions and used to coat MacConkey plates; the number of bacteria was quantified, and the viable cell count (CFU/g) was calculated.

2.13 Histopathological observation

A total of 40 (18–22 g weight, 6 weeks old) SPF KM mice (half of them male and half female) were randomly divided into four groups with ten mice in each group. The experiment was started 2 d after the mice were acclimated to the new environment. Group A was the wild-type GPKP strain group, Group B was the GPKP-Δ*kp05372* mutant group, Group C was the GPKP-Δ*kp05372*$^+$ complemented strain group, and Group D was the control group; ten mice were used in each group. The concentrations of bacterial solution of the wild-type GPKP, the GPKP-Δ*kp05372* mutant, and GPKP-Δ*kp05372*$^+$ complemented strains were 6.3×10^7, 1.1×10^{10}, and 4.88×10^9 CFU/mL, respectively, based on LD_{50} measurement after intraperitoneal injections at 0.5 mL per mouse. At 12, 48, and 96 h after injecting, three mice were killed for each group, and the heart, liver, spleen, lung, kidney, and intestine were collected. Meanwhile, pathological changes of each organ were observed by hematoxylin-eosin (HE) staining.

2.14 Statistical analysis

SPSS (Version 22.0) was used for data processing and analysis, and one-way analysis of variance (ANOVA) was used for determining statistical significance. $P<0.05$ indicated significant difference.

3 Results

3.1 Gene deletion mutation and complementation

For the *kp05372* upstream homologous arm fragment A, the total length of the PCR product was 638 bp. For the *kp05372* downstream homologous arm fragment B, the total length of the PCR product was 629 bp. For the fused fragment AB, the total length of the PCR product was 1267 bp. The length of the pLP12T-*kp05372* amplification product was 1517 bp and consistent with the expectation, indicating the successful construction of *E. coli* β2163 containing the suicide plasmid pLP12T-*kp05372*. The zygotes amplification product, using KP-M1F/KP-M2R as the primer pair, had two bands: one of the amplified fragments was 2077-bp long, and the other amplified band was 1267-bp long, which was consistent with the expected results. The mutant and wild-type amplification products, using KP-PF/KP-PR as the primer pair, are shown in Fig. 1. The correct mutant amplification produced a 1386-bp fragment, and the wild-type amplification produced a 2196-bp fragment. The PCR products and the sequencing results were consistent with the expectation.

The length of the expression fragment *kp05372* was 949 bp. The length of the pBAD33 vector fragment was 5529 bp. The amplification products of the recombinant clone pBAD33-*kp05372* are shown in lanes 1–2 in Fig. 2, and the length of the PCR products is 1053 bp; the sequencing results are consistent with the expectation. The amplification products of the donor bacteria *E. coli* β2163 containing pBAD33-*kp05372* are shown in lanes 3–4 in Fig. 2, and the amplification products of the GPKP-Δ*kp05372*$^+$ complemented strain are shown in lanes 5–6 in Fig. 2. The length of the PCR products is 1053 bp. The sequencing results of GPKP-Δ*kp05372*$^+$ complemented strain are consistent with expectation. It indicates that the GPKP-Δ*kp05372*$^+$ complemented strain was successfully constructed.

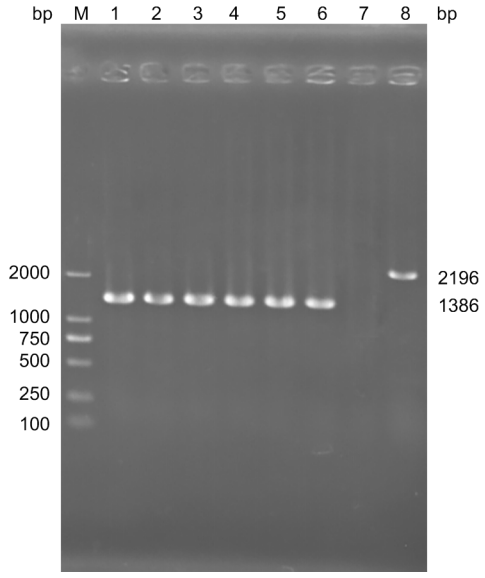

Fig. 1 Electrophoregram of the amplified fragments obtained from the GPKP-Δ*kp05372* mutation and wild-type strains

M: DL2000 DNA marker; 1–6: deletion mutant strains; 7: *E. coli* β2163 (pLP12T-*kp05372*); 8: wild-type strain

3.2 In vitro growth curves

As shown in Fig. 3, the growth rate of all the three strains showed a rapid rise in OD_{600} after 2 h and reached the maximum at 12 h. This period was in the exponential phase, when the OD_{600} value of the wild-type strain solution was higher than those of the other two strains. However, the plate counting results showed no significant change among the three strains.

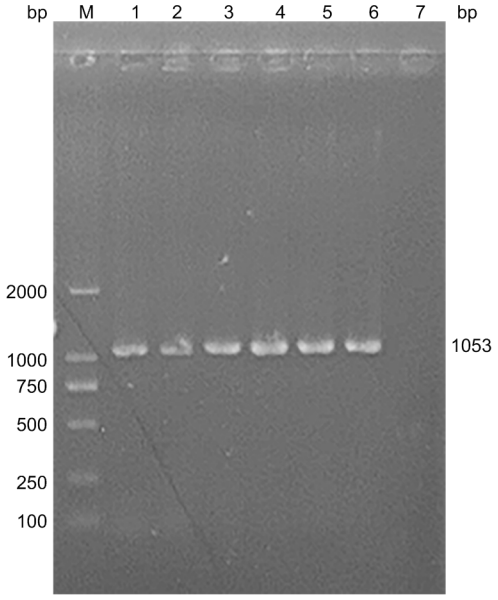

Fig. 2 Electrophoregram of amplified fragments obtained from pBAD33-*kp05372*, *E. coli* β2163 containing pBAD33-*kp05372,* and GPKP-Δ*kp05372*$^+$ complemented strains

M: DL2000 DNA marker; 1–2: pBAD33-*kp05372*; 3–4: *E. coli* β2163 containing pBAD33-*kp05372*; 5–6: GPKP-Δ*kp05372*$^+$ complemented strain; 7: GPKP-Δ*kp05372* mutant strain

The 12–18 h curve was relatively stable and in the stationary phase. After 18 h, the plate counting results showed that the curve gradually decreased and was in the death phase. The results of the OD_{600} values of the bacterial broth and the viable cell counts indicate that deletion of the *kp05372* gene does not affect the growth rate of GPKP.

3.3 Expression analysis of genes upstream of *kp05372*

Quantitative RT-PCR using specific primers was used to examine the expression of the genes upstream of *kp05372* in wild-type GPKP and GPKP-Δ*kp05372* mutant strains (Table 1). The results are shown in Fig. 4. Compared to the wild-type GPKP, expression of the *kp05372* upstream genes *kp05374*, *kp05378*, and *kp05379* showed a significant difference in the GPKP-Δ*kp05372* mutant (P<0.05). The GPKP-Δ*kp05372* mutant showed an increased expression for *kp05374* (to 1.32-fold) and *kp05379* (to 1.42-fold) and a decreased expression for *kp05378* (by 42%). No significant difference in expression level was observed for *kp05373*, *kp05375*, *kp05376*, or *kp05377*.

3.4 Biofilm formation assays

As shown in Table 2, the average value of the blank control is 0.127, plus three times the standard deviation, with the critical value T=0.169. Medium biofilm was formed in the wild-type and GPKP-Δ*kp05372*$^+$ complemented strains, and weak biofilm was formed in the GPKP-Δ*kp05372* mutant strains.

3.5 Drug sensitivity test

The results were interpreted according to CLSI (2019). The resistance of the GPKP-Δ*kp05372* mutant to cephalothin, compound sulfamethoxazole, and polymyxin B changed. As shown in Fig. 5, among the aminoglycosides, the inhibition zones of wild-type GPKP and GPKP-Δ*kp05372*$^+$ complemented strains grown on gentamicin and tobramycin were larger than that of the GPKP-Δ*kp05372* mutant, whereas the inhibition zone for the same when grown on neomycin and streptomycin was less than that of the GPKP-Δ*kp05372* mutant. Among the quinolones, both wild-type GPKP and GPKP-Δ*kp05372*$^+$ complemented strains had larger inhibition zones than the

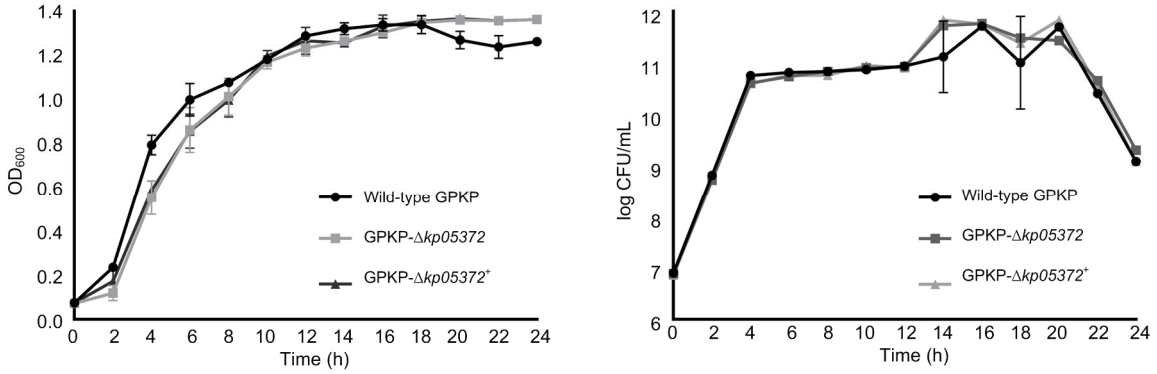

Fig. 3 Growth curves of wild-type GPKP, GPKP-Δ*kp05372* mutant, and GPKP-Δ*kp05372*$^+$ complemented strains

OD_{600}: optical density at 600 nm; CFU: colony-forming unit. Data are expressed as mean±standard deviation (n=3)

Table 2 Detection of biofilm absorption

Strain	OD_{570}			Average value	Standard deviation	Biofilm formation
	No. 1	No. 2	No. 3			
Wild-type	0.495	0.324	0.313	0.377	0.102	Medium
Mutant	0.403	0.271	0.309	0.327	0.068	Weak
Complemented	0.460	0.374	0.283	0.372	0.089	Medium
Blank	0.133	0.136	0.111	0.127	0.014	No

The critical value T was the mean OD_{570} value of the blank control plus three times its standard deviation. No biofilm forms when the sample's OD_{570} is less than or equal to T. Weak biofilm forms when the sample's OD_{570} is greater than T and less than 2T. Medium biofilm forms when the sample's OD_{570} is greater than 2T and less than 4T. Strong biofilm forms when the sample's OD_{570} is greater than 4T (Murphy and Kirkham, 2002)

GPKP-Δ*kp05372* mutant. Among the penicillins, the inhibition zones of wild-type GPKP and GPKP-Δ*kp05372*$^{+}$ complemented strains grown only on carbenicillin were larger than that for the GPKP-Δ*kp05372* mutant, and the results with the remaining drugs showed no difference. Among the cephalosporins, the inhibition zones of wild-type GPKP and GPKP-Δ*kp05372*$^{+}$ complemented strains grown only on cephalothin were larger than that of the GPKP-Δ*kp05372* mutant, while, for the remaining drugs, the inhibition zones of wild-type GPKP and GPKP-Δ*kp05372*$^{+}$ complemented strains were smaller than that of the GPKP-Δ*kp05372* mutant. Among the latter several antibiotics, the inhibition zones of wild-type GPKP and GPKP-Δ*kp05372*$^{+}$ complemented strains were larger than those of the GPKP-Δ*kp05372* mutant for compound sulfamethoxazole, furazolidone, chloramphenicol, and polymyxin B, while being smaller than the zones for erythromycin, tetracycline, and vancomycin.

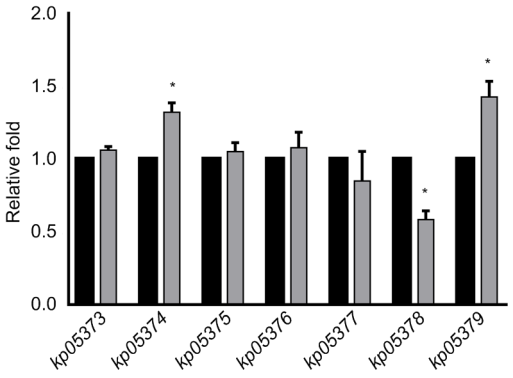

Fig. 4 Transcriptional levels of *kp05372* upstream genes *kp05373*, *kp05374*, *kp05375*, *kp05376*, *kp05377*, *kp05378*, and *kp05379*

Relative transcriptional levels of *kp05372* upstream genes in wild-type GPKP (black bars) and GPKP-Δ*kp05372* mutant (grey bars) strains determined using real-time RT-PCR are shown in comparison with the levels in the wild-type strain. The wild-type strain's expression level is represented as one fold. Each bar represents the mean value of three independent experiments. Error bars are standard deviations.* Significant difference (P<0.05)

Briefly, the antibiotic sensitivities of wild-type GPKP strain and GPKP-Δ*kp05372*$^{+}$ complemented strain are similar. The inhibition zone diameters of the GPKP-Δ*kp05372* mutant grown on gentamicin, ofloxacin, cephalothin, compound sulfamethoxazole, furazolidone, chloramphenicol, and polymyxin B were smaller by >5 mm compared to those of the wild-type GPKP and the GPKP-Δ*kp05372*$^{+}$ complemented strains, and the diameter of the inhibition zone for cells grown on neomycin was larger by >5 mm compared to those of the wild-type GPKP strain and the GPKP-Δ*kp05372*$^{+}$ complemented strain. However, only the changes for neomycin, cephalothin, compound sulfamethoxazole, furazolidone, and polymyxin B reached the sensitive points required by CLSI (2019).

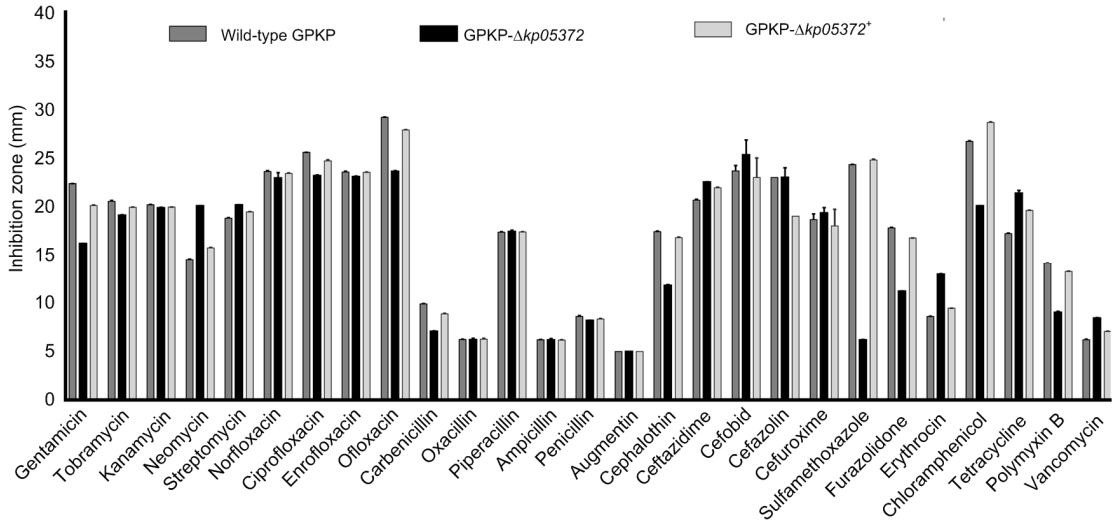

Fig. 5 Diameters of inhibition zones of the wild-type GPKP, GPKP-Δ*kp05372* mutant, and GPKP-Δ*kp05372*$^{+}$ complemented strains

Each bar represents the mean value of three independent experiments. Error bars are standard deviations

3.6 Stress sensitivity assay

As shown in Fig. 6, compared with the other two strains, the OD_{600} value of the GPKP-Δ*kp05372* mutant was significantly increased by about 0.3 times at pH 2, and the log value of the viable cell count was significantly increased by about 0.4 times. At pH 3, the OD_{600} value and the log value of the viable cell count of the GPKP-Δ*kp05372* mutant were increased by about 0.2 times. At pH 5, the OD_{600} value of the GPKP-Δ*kp05372* mutant was increased by about 0.15 times, while the viable cell count results showed no significant change. To sum up, combined with the OD_{600} value and the viable cell count results of the three strains, the acid tolerance of the GPKP-Δ*kp05372* mutant decreased gradually with increase in pH value, with the alkali tolerance showing no obvious change; the three strains showed no significant change in terms of resistance to osmotic pressure, salt tolerance, oxidation resistance, or temperature sensitivity.

3.7 Infection of SPF KM mice

Twelve hours after the challenge experiment, the mice became dispirited and showed symptoms such as low appetite for food, messy hair, and secretions at the corners of the eyes; the mice gradually died after 24 h. The mice in the control group had normal mental activity and appetite for food, and no significant abnormality was found in the autopsy. Seven days after injection, LD_{50} was calculated by the Bliss method. LD_{50} values of the GPKP-Δ*kp05372* mutant and GPKP-Δ*kp05372*$^+$ complemented strains were 1.1×10^{10} and 4.9×10^9 CFU/mL, respectively. Compared with LD_{50} of GPKP (6.3×10^7 CFU/mL) (Zhao et al., 2017b), the virulence of GPKP-Δ*kp05372* mutant was found to be decreased significantly.

3.8 Organ colonization assays

Except the lungs, the colonization abilities of the GPKP-Δ*kp05372* mutant in the heart, liver, spleen, kidney, and intestine were the weakest, and the bacterial content could not be detected at the earliest. As shown in Fig. 7a, the content of the GPKP-Δ*kp05372* mutant in the heart was about 10% of wild-type GPKP and GPKP-Δ*kp05372*$^+$ complemented strains, and the time to reduce the content to zero was significantly earlier than that of the latter two strains. As shown in Fig. 7b, the content of wild-type GPKP in the liver was always about 15 times higher than that of GPKP-Δ*kp05372*$^+$ complemented strains. The content of the GPKP-Δ*kp05372* mutant was the same as that of the wild-type GPKP at 12 and 24 h, while being the same as GPKP-Δ*kp05372*$^+$ complemented strains at 48 and 72 h. The colonization ability of the GPKP-Δ*kp05372* mutant was significantly decreased. As shown in Fig. 7c, in the spleen, the content of wild-type GPKP and GPKP-Δ*kp05372* mutant was the same at 12 and 24 h, which was 12 and 27 times higher than that of the GPKP-Δ*kp05372*$^+$ complemented strains, respectively. After 48 h, the content of the three strains was significantly decreased, and no GPKP-Δ*kp05372* mutant was detected. Therefore, the colonization ability of the GPKP-Δ*kp05372* mutant was weaker. As shown in Fig. 7d, in the lungs, the amount of colonization of wild-type GPKP and GPKP-Δ*kp05372* mutant at 24 h was the same, 685 times as that of the GPKP-Δ*kp05372*$^+$ complemented strains. The content of the GPKP-Δ*kp05372* mutant at 48 h

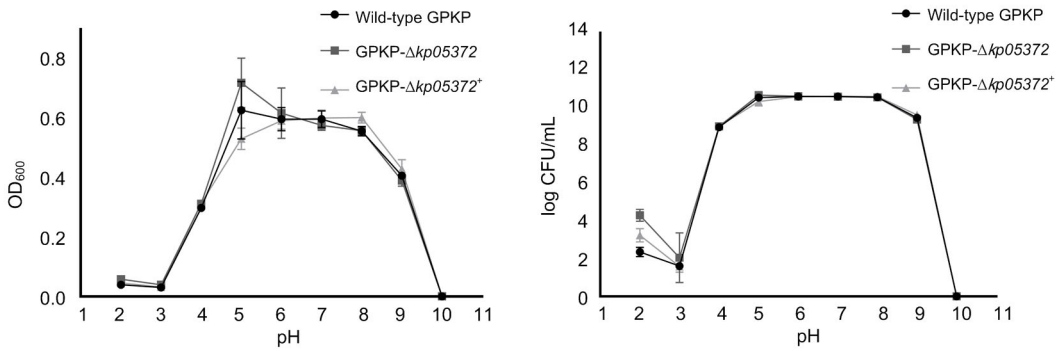

Fig. 6 Acidity-alkalinity sensitivity curves of the wild-type GPKP, GPKP-Δ*kp05372* mutant, and GPKP-Δ*kp05372*$^+$ complemented strains

OD_{600}: optical density at 600 nm; CFU: colony-forming unit. Data are expressed as mean±standard deviation (n=3)

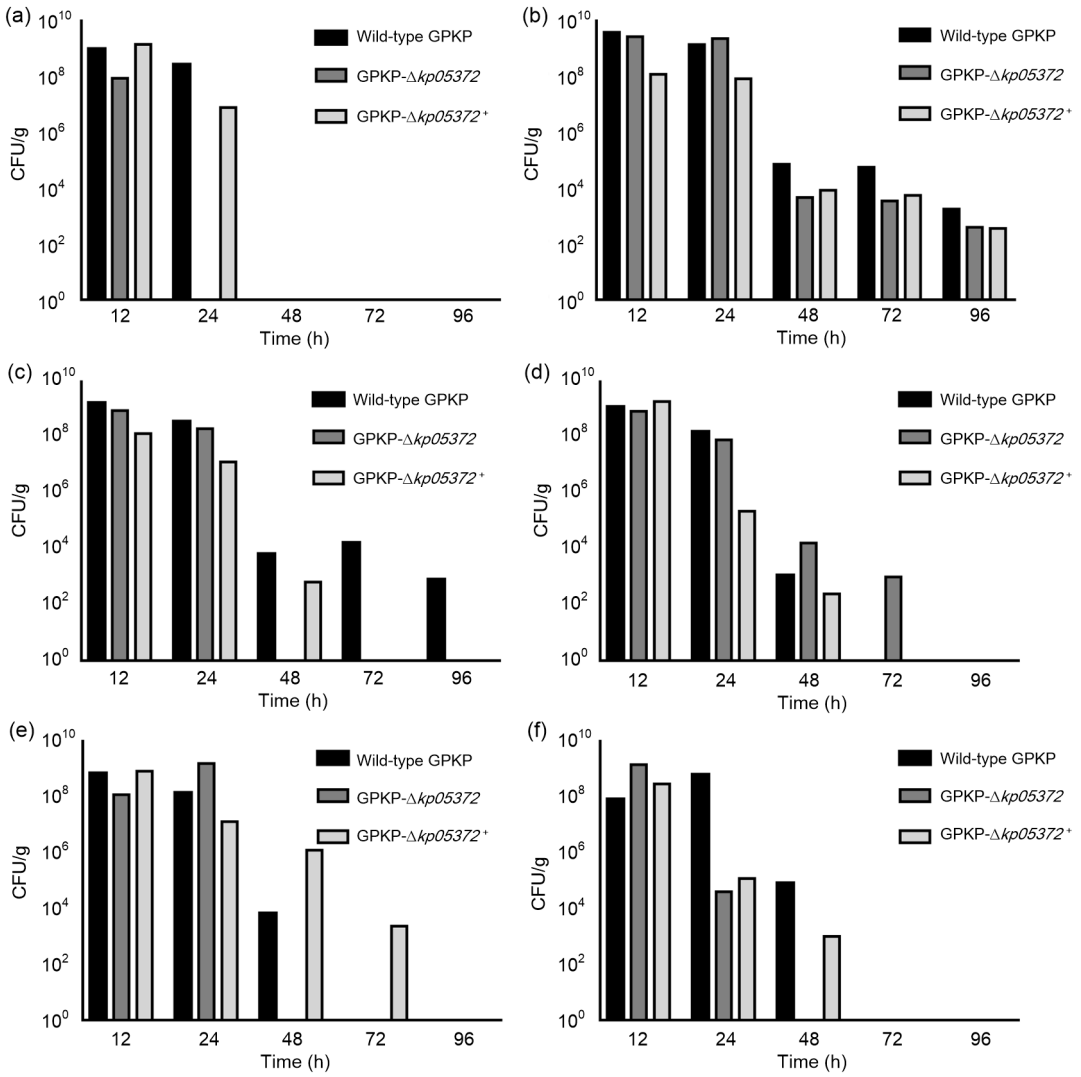

Fig. 7 Organ colonization amount of the wild-type GPKP, GPKP-Δ*kp05372* mutant, and *GPKP-Δkp05372*$^+$
The colonization of the heart (a), liver (b), spleen (c), lung (d), kidney (e), and intestine (f). CFU: colony-forming unit

was higher than that of the wild-type GPKP and GPKP-Δ*kp05372*$^+$ complemented strains, and the colonization ability of the GPKP-Δ*kp05372* mutant was stronger. As shown in Fig. 7e, at 24 h, in the kidney, the content of the GPKP-Δ*kp05372* mutant increased to 17 times that of the wild-type GPKP, and the colonization ability of the GPKP-Δ*kp05372* mutant was enhanced. At 48 h, the content of the GPKP-Δ*kp05372* mutant was not detected, the amount of colonization of the GPKP-Δ*kp05372*$^+$ complemented strains was 187 times that of the wild-type GPKP, and the colonization ability of the GPKP-Δ*kp05372* mutant decreased more significantly than that of the wild-type GPKP. As shown in Fig. 7f, in the intestinal tract, the colonization amount of wild-type GPKP at 24 h was 15750 times that of the GPKP-Δ*kp05372* mutant and 5250 times that of the GPKP-Δ*kp05372*$^+$ complemented strains. The wild-type GPKP had the strongest colonization ability. The GPKP-Δ*kp05372* mutant was not detected at 48 h, and the decrease in the colonization ability of the GPKP-Δ*kp05372* mutant was more obvious than that of the wild-type GPKP.

3.9 Histopathological observation

There were no significant pathological changes in the cardiac tissue. The pathological changes in

spleen, kidney, and intestine were consistent. Liver and lung showed different histopathological changes at 96 h. At 12 h, hepatocyte injury showed central venous congestion, peripheral lymphocytic infiltration, hepatic sinus stricture, and unclear hepatic cord structure. In the GPKP-Δ*kp05372* mutant and GPKP-Δ*kp05372*$^+$ groups, individual binuclear hepatocytes with densely stained cytoplasm were observed (Figs. 8g and 8j). At 48 h, a small number of small vacuoles in the cytoplasm of some hepatocytes were observed. At 96 h, hepatocytes in the wild-type GPKP group were swollen (Fig. 8f), and hepatocytes in the GPKP-Δ*kp05372*$^+$ group were lysed (Fig. 8l), all of which indicated liver cell degeneration. The liver cell structure in the GPKP-Δ*kp05372* mutant group was complete, and a large number of proliferating spindle or polygonal Kupffer cells were observed (Fig. 8i). At 12 h, the congestion of the alveolar capillaries was observed in the GPKP-Δkp05372 mutant and GPKP-Δ*kp05372*$^+$ groups, and the lung interval was significantly thickened (Figs. 9g and 9j). A small amount of inflammatory cell infiltration was observed in wild-type GPKP group (Fig. 9d). At 48 h, local alveolar septum atrophy was observed, with inflammatory cell infiltration, and a small amount of exudate was observed in the alveolar cavity of the GPKP-Δ*kp05372*$^+$groups (Figs. 9e, 9h, and 9k). At 96 h, a large number of red blood cells and inflammatory cells had infiltrated, and alveolar cell degeneration was observed in the GPKP-Δ*kp05372* mutant group (Fig. 9i). The alveolar structure of the wild-type GPKP and GPKP-Δ*kp05372*$^+$ groups was relatively complete, and the local alveolar septum was atrophic (Figs. 9f and 9l).

4 Discussion

The forest musk deer is a protected animal in China and is listed as “endangered” with the International Union for Conservation of Nature. Musk secreted by the musk glands of adult male musk deer

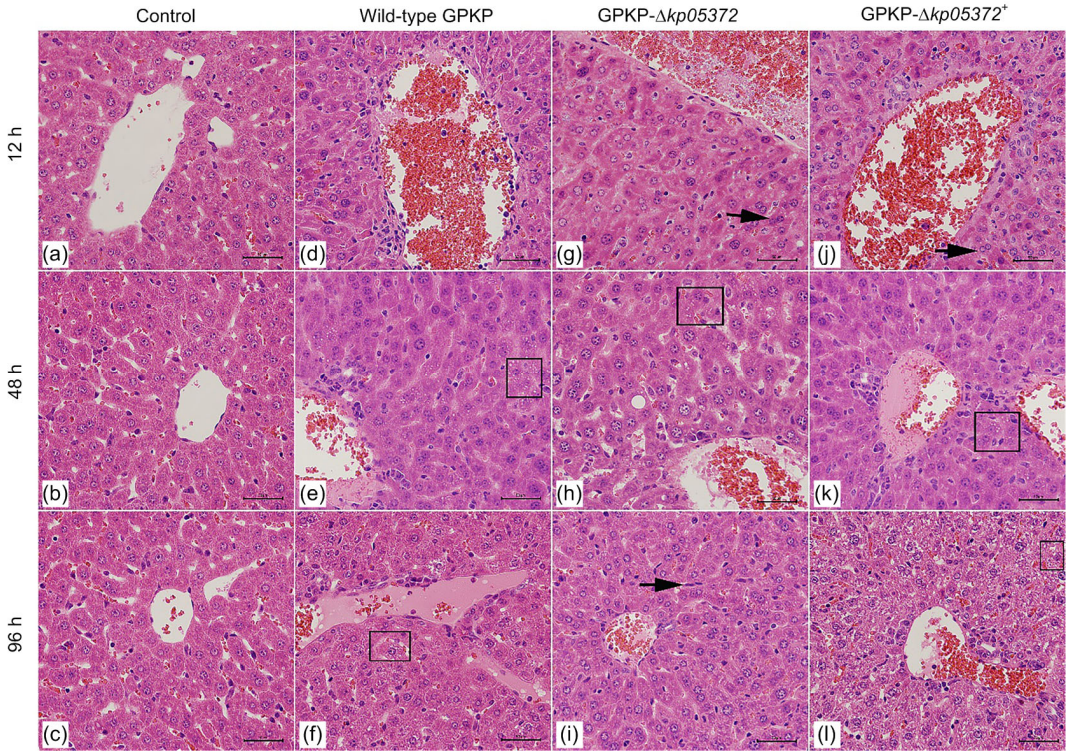

Fig. 8 Micrographs of liver tissues in the wild-type GPKP, GPKP-Δ*kp05372* mutant, and GPKP-Δ*kp05372*$^+$ groups at 12, 48, and 96 h (HE stain, ×400)

Micrographs of liver tissues of the control group at 12 h (a), 48 h (b), and 96 h (c). Micrographs of liver tissues in the wild-type GPKP group at 12 h (d), 48 h (e), and 96 h (f); Micrographs of liver tissues in the GPKP-Δ*kp05372* mutant group at 12 h (g), 48 h (h), and 96 h (i). Micrographs of liver tissues in the GPKP-Δ*kp05372*$^+$ group at 12 h (j), 48 h (k), and 96 h (l). (d, e, h, k) □: small vacuole; (f) □: hepatocyte swelling; (g, j) →: binuclear hepatocyte; (i) →: Kupffer cell; (l) □: hepatocyte lysis. Scale bar=50 μm

has an important economic value in traditional Asian medicine and international perfume industries (Yang et al., 2003; Zhao et al., 2017a). GPKP is a threat to the captive breeding of musk deer. It is important to study GPKP for the protection of musk deer and for the exploitation and utilization of musk resources. Study of the effect of the novel LysR transcription factor gene *kp05372* on GPKP aims to provide new clues for the clinical prevention and treatment of GPKP, as well as provide new references for the study of LysR transcription factors.

In this study, we successfully constructed the *kp05372* gene deletion and the complemented strains. In the follow-up experiments, the complemented strain could largely restore the changes caused by gene deletion and, thus, eliminate the polar effect of gene deletion mutations. Quantitative RT-PCR was performed on seven potential target genes upstream of *kp05372*, which showed a certain regulatory effect on the expression of *kp05374*, *kp05378*, and *kp05379*, consistent with the characteristics of the LysR family genes that are adjacent and opposite to their target genes. These results provide evidence for the additional regulatory role of *kp05372* on the expression level of its upstream genes. The differential expression of these genes could be the molecular mechanism underlying the biological and phenotypic change in the GPKP-Δ*kp05372* mutant used in this study.

The process of bacterial growth consists of four phases, in which bacteria die and regenerate. It is impossible to distinguish dead bacteria from living bacteria by simply measuring the absorbance value of the bacterial solution. Therefore, counting of the viable cells of the bacterial solution was also carried out at the same time, and the combination of the two methods could compare the growth profiles of the three strains of bacteria better. The OD value measured in this experiment was basically consistent with

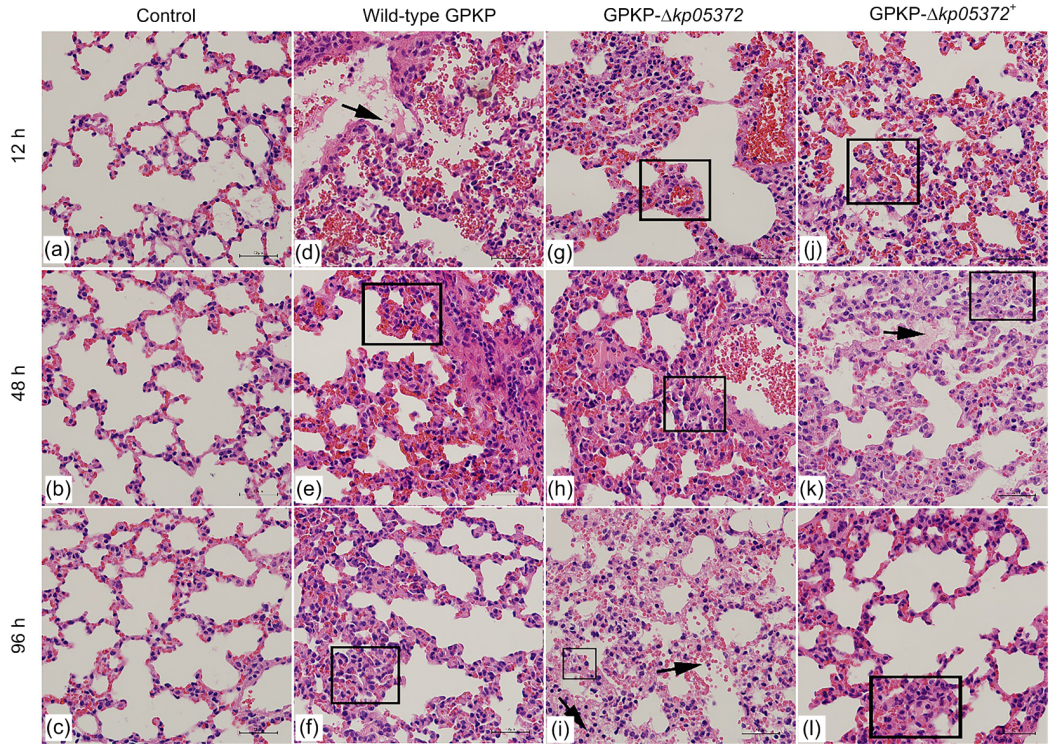

Fig. 9 Micrographs of lung tissues in the wild-type GPKP, GPKP-Δ*kp05372* mutant, and GPKP-Δ*kp05372*$^+$ groups at 12, 48, and 96 h (HE stain, ×400)

Micrographs of lung tissues of the control group at 12 h (a), 48 h (b), and 96 h (c). Micrographs of lung tissues in the wild-type GPKP group at 12 h (d), 48 h (e), and 96 h (f). Micrographs of lung tissues in the GPKP-Δ*kp05372* mutant group at 12 h (g), 48 h (h), and 96 h (i). Micrographs of lung tissues in the GPKP-Δ*kp05372*$^+$ group at 12 h (j), 48 h (k), and 96 h (l). (d) →: inflammatory cells; (e) □: pulmonary septal thickening, congestion of the alveolar capillaries; (f, h, l) □: alveolar septum atrophy; (g, j) □: pulmonary septal thickening, capillary injection; (i) □: alveolar cell degeneration; →: inflammatory cells and red blood cells; (k) □: alveolar septum atrophy; →: inflammatory exudate. Scale bar=50 μm

the conclusion obtained from the count of viable bacteria before the death phase. After 20 h, all the three strains were in the death phase. At this time, due to the large number of dead bacteria in the solution, the OD value was different from the count of viable bacteria. Therefore, more attention should be paid to the count of viable bacteria. At 2, 4, and 6 h, the OD_{600} value of the wild-type GPKP strain solution was significantly higher than that of the GPKP-Δ*kp05372* mutant, and the values at 4, 6, and 8 h were significantly higher than that of the GPKP-Δ*kp05372*$^{+}$ complemented strain. However, the results of viable cell count showed that there was no significant change in the three strains, which might have been caused by the faster metabolism rate of the wild-type GPKP strain and the higher content of dead bacteria. The measured data of the GPKP-Δ*kp05372*$^{+}$ complemented strain were slightly higher than those of the GPKP-Δ*kp05372* mutant strain, which might have been caused by the low expression of the complement gene. To sum up, gene deletion basically does not affect the growth rate of GPKP.

Biofilm, a kind of bacterial membrane-like aggregate, is formed by small colonies of bacteria that adhere to some surfaces and encapsulated by a polysaccharide matrix (Macfarlane, 2008). Biofilms of bacteria can increase resistance to antibiotics, heat stress, and pH (Wang et al., 2018). The ability to form biofilms is also related to the pathogenicity and drug resistance of *K. pneumoniae* (Lavender et al., 2004). The results of the biofilm formation assays showed that the wild-type GPKP strain and the GPKP-Δ*kp05372*$^{+}$ complemented strain formed medium biofilms and that the GPKP-Δ*kp05372* mutant formed a weak biofilm. The biofilm formation ability of GPKP decreased, and the reasons affecting the biofilm formation of GPKP might be related to capsular polysaccharide, adhesion factor, lipopolysaccharide, and extracellular DNA (Cramton et al., 1999; Whitchurch et al., 2002; de Araujo et al., 2010; Diago-Navarro et al., 2014; Dos Santos Goncalves et al., 2014; Vuotto et al., 2017). In addition, there is a relationship between the quorum sensing of bacteria and biofilm formation. Quorum sensing regulates adhesion, biofilm formation, accumulation of biofilm biomass, biofilm structure, and dispersion of biofilm cells (da Silva et al., 2017). The quorum sensing of *K. pneumoniae* regulates biofilm formation by secreting signal molecules associated with brominated furanone (AI-2) (Balestrino et al., 2005; de Araujo et al., 2010; Liu et al., 2016). Some LysR family genes have been reported to play the role of regulating the expression of quorum sensing-related genes (Cao et al., 2001; Sperandio et al., 2002; Kim et al., 2004). Therefore, it is speculated that the decrease in biofilm formation ability of the GPKP-Δ*kp05372* mutant may be related to the role of *kp05372* in regulating quorum sensing-related genes.

Bacterial resistance can be divided into natural resistance (determined by chromosomal genes) and acquired resistance (determined by plasmids). The mechanisms of *K. pneumoniae* resistance include the production of enzymes that inactivate antimicrobial agents, change of target sites of antimicrobial agents, decrease in permeability of antimicrobial agents, and changes in bacterial metabolic pathways (Yao et al., 2018; Yuan et al., 2018). The results of the drug sensitivity test indicated that gene deletion caused some changes in GPKP resistance. It is speculated that the cause of changes in drug resistance may be related to the formation of efflux pumps and biofilms. The efflux pump is a very important cause of bacterial resistance. It has been reported that the LysR family may affect the expression level of efflux pumps and thus affect the degree of bacterial resistance (Yang et al., 2017). Biofilm is also an important factor affecting the drug resistance of *K. pneumoniae*. Biofilms formed by bacteria can slow down the penetration of antibiotics and prevent antibiotics from entering the bacteria. The ability of an antibiotic to penetrate a biofilm depends on the rate of its inactivation in the biofilm (Anderl et al., 2000; Yang and Zhang, 2008). Therefore, changes in the capacity for biofilm formation may be an important cause for the changes in drug resistance in the GPKP-Δ*kp05372* mutant.

K. pneumoniae is found in the gastrointestinal tract of humans and animals, as well as in the environment. Hennequin and Forestier (2009) have reported that the colonization of the gastrointestinal tract by *K. pneumoniae* was a staged step to cause infection. The colonization of *K. pneumoniae* in the intestinal tract depends on its adhesion to the mucosa, its ability to form biofilms in the mucus, and its ability to resist various pressures encountered in the gastrointestinal tract (Wang et al., 2010; Zhou et al., 2013). Therefore, this experiment studied the tolerance of

wild-type GPKP, GPKP-Δ*kp05372* mutant, and GPKP-Δ*kp05372*$^+$ complemented strains under different conditions. The results of the pH sensitivity test indicate that deletion of the gene *kp05372* increases the acid resistance of GPKP, and the stronger the acid, the better is the acid resistance. This is similar to the experimental results of Huang et al. (2016). In addition, the activity of AI-2, the quorum sensing signal molecule of *K. pneumoniae*, has been reported to be variable in different acidic environments (Zhu et al., 2012). Signal generation is enhanced with high osmotic pressure as well as at low pH, when there is nutrient abundance (Balestrino et al., 2005). In addition to the effects of the growth environment, the LysR family of transcription factors themselves may also play a role in regulating quorum sensing.

The lethality of the GPKP-Δ*kp05372* mutant strain was 1.1×10^{10} CFU/mL, which was significantly different from that of the wild-type GPKP strain measured earlier in the laboratory, which was 6.3×10^{7} CFU/mL, and significantly higher than that of the GPKP-Δ*kp05372*$^+$ complemented strain. It is speculated that the virulence of the wild-type GPKP strain became relatively weak after gene deletion, which affected the pathogenicity of GPKP.

K. pneumoniae infection is based on the colonization of the respiratory and intestinal tracts. Bacterial colonization is related to its own level of adhesion. After a challenge, bacteria need to face different nutritional conditions, pH environments, and the resistance of cells of the various organs to their reproduction in mice; a large number of bacteria will gradually reduce to either no colonization or stable bacterial colonization and may even cause infection. In the experiment on colonization of mouse organs by three strains of bacteria, the time when the organ colonization amount decreased the most was found to be generally 24–48 h, and the content of bacteria in the heart, spleen, kidney, and intestinal tract of the GPKP-Δ*kp05372* mutant strain first decreased to zero, which might be related to the immune response of the body and the role of phagocytes. In the heart, liver, kidney, and intestine, the colonization abilities of wild-type strains were the strongest, and colonization always existed in the liver. It was speculated that the deletion of gene *kp05372* affected the adhesion ability of the GPKP-Δ*kp05372* mutant strain, and the colonization ability in the organ decreased, which was consistent with the results showing increased LD_{50} and decreased virulence of the GPKP-Δ*kp05372* mutant strain. In addition, biofilm formation assays found that the biofilm formation ability of the GPKP-Δ*kp05372* mutant strain was reduced and its resistance to the external environment was weakened, which might also affect the colonization ability of GPKP in organs.

From colonization to infection to tissue lesion, bacteria have different processes according to individuals and objects. There were obvious hepatic histopathological changes after challenge by the wild-type GPKP strain, the GPKP-Δ*kp05372* mutant strain, and the GPKP-Δ*kp05372*$^+$ complemented strain; however, in the GPKP-Δ*kp05372* mutant group, there were not only cytoplasmic hyperchromatic and binuclear hepatocytes with pyknotic nuclei, but also a large number of Kupffer cells. Binuclear hepatocytes suggest that hepatocytes have strong regeneration ability. Kupffer cells are a type of liver macrophages, and the abundance of Kupffer cells can provide a stronger defense against bacteria (Li and Ji, 2017). The structure of mouse hepatocytes in the GPKP-Δ*kp05372* mutant group was more complete than that in the other two groups, and the wild-type GPKP strain and the GPKP-Δ*kp05372*$^+$ complemented strain had more damage to the liver cells. The damage caused by bacteria to spleen cells in the three groups was relatively consistent. A large number of megakaryocytes could be seen in the three groups 48 and 96 h after challenge, suggesting that extramedullary hematopoiesis might occur, which might be caused by hypersplenism after bacterial infection (Zhai and Wang, 2017). Pulmonary septal thickening, severe hyperemia of the capillaries in the alveolar walls, and infiltration by a large number of inflammatory cells were observed at 12 h after challenge (Cai et al., 2009). At 48 and 96 h after challenge, the pulmonary septum gradually returned to normal in the wild-type GPKP strain group and the GPKP-Δ*kp05372*$^+$ complemented strain group, and the degree of capillary hyperemia was weakened. After challenge, severe histopathological changes firstly appeared in the intestinal tract of the GPKP-Δ*kp05372* mutant strain group, with a large number of intestinal villi shedding, edema of the epithelial mucosal cells, and a large amount of degeneration and necrosis. Complete intestinal villi were observed 48 h after challenge. In clinical

practice, *K. pneumoniae* has been found to mainly affect the respiratory and intestinal organs, which is consistent with the results of organ colonization.

In conclusion, the *kp05372* gene could partially regulate seven adjacent upstream genes. The deletion of *kp05372* reduced the biofilm formation ability and, at the same time, changed the drug resistance, colonization ability, and virulence of bacteria. The decrease in biofilm formation ability might indirectly affect the drug resistance, adhesion, and virulence of bacteria. In addition, the deletion of *kp05372* also had some impact on the acid resistance ability of bacteria. Apart from the effect on biofilm formation, the effect of LysR family of transcriptional regulators on the quorum sensing ability of *K. pneumoniae* might also be related to the effect on acid resistance. At present, we have studied the function of *kp05372* in determining the biological characteristics of GPKP. Next, we will further study the functions of this gene in bacterial quorum sensing and related drug resistance mechanism so as to provide valuable help for the actual treatment, prevention, and control of diseases.

Contributors

Wei YANG, Wu-you WANG, and Yan LUO designed the experiment. Wei YANG and Wu-you WANG wrote the paper. Wu-you WANG carried out gene knockout and complementation experiments and other bacterial in vitro experiments. Wei YANG and Wei ZHAO performed animal experiments and quantitative RT-PCR analysis, and Dong YU provided assistance for the experiment. Yan LUO, Jian-guo CHENG, Yin WANG, Xue-ping YAO, and Ze-xiao YANG gave assistance for the experiment and made suggestions on the content of the manuscript. All authors have full access to all data in the study and are responsible for the integrity and security of the data.

Acknowledgments

We thank the Animal Quarantine Laboratory of the College of Veterinary Medicine of Sichuan Agricultural University (Wenjiang, China) for providing experimental conditions for the experiment. We also thank Guangzhou KnoGen Biotech Co., Ltd. for providing help for the experiment. We extend our thanks to the hard work of the experimental contributors.

Compliance with ethics guidelines

Wei YANG, Wu-you WANG, Wei ZHAO, Jian-guo CHENG, Yin WANG, Xue-ping YAO, Ze-xiao YANG, Dong YU, and Yan LUO declare that they have no conflict of interest.

All institutional and national guidelines for the care and use of laboratory animals were followed and animal experiments were approved by the National Institute of Animal Health Care and Use Committee at Sichuan Agricultural University (approval number SYXK2019-187).

References

Anderl JN, Franklin MJ, Stewart PS, 2000. Role of antibiotic penetration limitation in *Klebsiella pneumoniae* biofilm resistance to ampicillin and ciprofloxacin. *Antimicrob Agents Chemother*, 44(7):1818-1824. https://doi.org/10.1128/aac.44.7.1818-1824.2000

Balestrino D, Haagensen JAJ, Rich C, et al., 2005. Characterization of type 2 quorum sensing in *Klebsiella pneumoniae* and relationship with biofilm formation. *J Bacteriol*, 187(8):2870-2880. https://doi.org/10.1128/jb.187.8.2870-2880.2005

Bliss CI, 1935. The calculation of the dosage-mortality curve. *Ann Appl Biol*, 22(1):134-167. https://doi.org/10.1111/j.1744-7348.1935.tb07713.x

Bujanda L, Cosme A, Beguiristaín A, et al., 1996. Multiple liver abscesses, peritonitis and acute enteritis caused by *Klebsiella pneumoniae*. *Gastroenterol Hepatol*, 19(6):336-337.

Cai SS, Batra S, Shen L, et al., 2009. Both TRIF- and MyD88-dependent signaling contribute to host defense against pulmonary *Klebsiella* infection. *J Immunol*, 183(10):6629-6638. https://doi.org/10.4049/jimmunol.0901033

Cao H, Krishnan G, Goumnerov B, et al., 2001. A quorum sensing-associated virulence gene of *Pseudomonas aeruginosa* encodes a LysR-like transcription regulator with a unique self-regulatory mechanism. *Proc Natl Acad Sci USA*, 98(25):14613-14618. https://doi.org/10.1073/pnas.251465298

CLSI (Clinical and Laboratory Standards Institute), 2019. Drug Sensitivity Test Implementation Standards; Twenty-Ninth Edition Information Supplement. CLSI Document M100, p.93-96.

Cramton SE, Gerke C, Schnell NF, et al., 1999. The intercellular adhesion (*ica*) locus is present in *Staphylococcus aureus* and is required for biofilm formation. *Infect Immun*, 67(10):5427-5433.

da Silva DP, Schofield MC, Parsek MR, et al., 2017. An update on the sociomicrobiology of quorum sensing in Gram-negative biofilm development. *Pathogens*, 6(4):51. https://doi.org/10.3390/pathogens6040051

de Araujo C, Balestrino D, Roth L, et al., 2010. Quorum sensing affects biofilm formation through lipopolysaccharide synthesis in *Klebsiella pneumoniae*. *Res Microbiol*, 161(7):595-603. https://doi.org/10.1016/j.resmic.2010.05.014

Diago-Navarro E, Chen L, Passet V, et al., 2014. Carbapenem-resistant *Klebsiella pneumoniae* exhibit variability in capsular polysaccharide and capsule associated virulence traits. *J Infect Dis*, 210(5):803-813. https://doi.org/10.1093/infdis/jiu157

Dos Santos Goncalves M, Delattre C, Balestrino D, et al., 2014. Anti-biofilm activity: a function of *Klebsiella pneumoniae*

capsular polysaccharide. *PLoS ONE*, 9(6):e99995. https://doi.org/10.1371/journal.pone.0099995

Fang CT, Chuang YP, Shun CT, et al., 2004. A novel virulence gene in *Klebsiella pneumoniae* strains causing primary liver abscess and septic metastatic complications. *J Exp Med*, 199(5):697-705. https://doi.org/10.1084/jem.20030857

Frisch RL, Bender RA, 2010. Expanded role for the nitrogen assimilation control protein in the response of *Klebsiella pneumoniae* to nitrogen stress. *J Bacteriol*, 192(19): 4812-4280. https://doi.org/10.1128/JB.00931-09

He K, Xin YP, Shan Y, et al., 2019. Phosphorylation residue T175 in RsbR protein is required for efficient induction of sigma B factor and survival of listeria monocytogenes under acidic stress. *J Zhejiang Univ-Sci B (Biomed & Biotechnol)*, 20(8):660-669. https://doi.org/10.1631/jzus.B1800551

Henikoff S, Haughn GW, Calvo JM, et al., 1988. A large family of bacterial activator proteins. *Proc Natl Acad Sci USA*, 85(18):6602-6606. https://doi.org/10.1073/pnas.85.18.6602

Hennequin C, Forestier C, 2009. OxyR, a LysR-type regulator involved in *Klebsiella pneumoniae* mucosal and abiotic colonization. *Infect Immun*, 77(12):5449-5457. https://doi.org/10.1128/IAI.00837-09

Huang FY, Ding XM, Lin YL, et al., 2016. Study on the influence of environmental factors on the growth of *Klebsiella pneumoniae*. *Med Forum*, 20(36):5136-5137 (in Chinese). https://doi.org/10.19435/j.1672-1721.2016.36.044

Kim J, Kim JG, Kang Y, et al., 2004. Quorum sensing and the LysR-type transcriptional activator ToxR regulate toxoflavin biosynthesis and transport in *Burkholderia glumae*. *Mol Microbiol*, 54(4):921-934. https://doi.org/10.1111/j.1365-2958.2004.04338.x

Lavender HF, Jagnow JR, Clegg S, 2004. Biofilm formation in vitro and virulence in vivo of mutants of *Klebsiella pneumoniae*. *Infect Immun*, 72(8):4888-4890. https://doi.org/10.1128/IAI.72.8.4888-4890.2004

Lederman ER, Crum NF, 2005. Pyogenic liver abscess with a focus on *Klebsiella pneumoniae* as a primary pathogen: an emerging disease with unique clinical characteristics. *Am J Gastroenterol*, 100(2):322-331. https://doi.org/10.1111/j.1572-0241.2005.40310.x

Lee S, Kim B, Jeong D, et al., 2013. Observation of 2,3-butanediol biosynthesis in Lys regulator mutated *Klebsiella pneumoniae* at gene transcription level. *J Biotechnol*, 168(4):520-526. https://doi.org/10.1016/j.jbiotec.2013.09.015

Li J, Ji JL, 2017. Liver macrophages: role in liver injury. *World Chin J Digestol*, 25(14):1223-1230 (in Chinese). https://doi.org/10.11569/wcjd.v25.i14.1223

Liu L, Gui M, Wu RY, et al., 2016. Progress in research on biofilm formation regulated by Luxs/AI-2 quorum sensing. *Food Sci*, 37(19):254-262 (in Chinese). https://doi.org/10.7506/spkx1002-6630-201619043

Macfarlane S, 2008. Microbial biofilm communities in the gastrointestinal tract. *J Clin Gastroenterol*, 42(S3):S142-S143. https://doi.org/10.1097/MCG.0b013e31816207df

Maddocks SE, Oyston PCF, 2008. Structure and function of the LysR-type transcriptional regulator (LTTR) family proteins. *Microbiology*, 154(12):3609-3623. https://doi.org/10.1099/mic.0.2008/022772-0

Murphy TF, Kirkham C, 2002. Biofilm formation by non-typeable *Haemophilus influenzae*: strain variability, outer membrane antigen expression and role of pili. *BMC Microbiol*, 2:7. https://doi.org/10.1186/1471-2180-2-7

O'Toole G, Kaplan HB, Kolter R, 2000. Biofilm formation as microbial development. *Ann Rev Microbiol*, 54:49-79. https://doi.org/10.1146/annurev.micro.54.1.49

Pfaffl MW, 2001. A new mathematical model for relative quantification in real-time RT-PCR. *Nucleic Acids Res*, 29(9):e45. https://doi.org/10.1093/nar/29.9.e45

Pollak CN, Wanke MM, Estein SM, et al., 2015. Immunization with *Brucella* virB proteins reduces organ colonization in mice through a Th1-type immune response and elicits a similar immune response in dogs. *Clin Vaccine Immunol*, 22(3):274-281. https://doi.org/10.1128/CVI.00653-14

Roberts DE, McClain HM, Hansen DS, et al., 2000. An outbreak of *Klebsiella pneumoniae* infection in dogs with severe enteritis and septicemia. *J Vet Diagn Invest*, 12(2): 168-173. https://doi.org/10.1177/104063870001200215

Sperandio V, Li CC, Kaper JB, 2002. Quorum-sensing *Escherichia coli* regulator A: a regulator of the LysR family involved in the regulation of the locus of enterocyte effacement pathogenicity island in enterohemorrhagic *E. coli*. *Infect Immun*, 70(6):3085-3093. https://doi.org/10.1128/IAI.70.6.3085-3093.2002

Srinivasan VB, Mondal A, Venkataramaiah M, et al., 2013. Role of $oxyR^{KP}$, a novel LysR-family transcriptional regulator, in antimicrobial resistance and virulence in *Klebsiella pneumoniae*. *Microbiology*, 159(7):1301-1314. https://doi.org/10.1099/mic.0.065052-0

Viswanathan P, Ueki T, Inouye S, et al., 2007. Combinatorial regulation of genes essential for *Myxococcus xanthus* development involves a response regulator and a LysR-type regulator. *Proc Natl Acad Sci USA*, 104(19):7969-7974. https://doi.org/10.1073/pnas.0701569104

Vuotto C, Longo F, Pascolini C, et al., 2017. Biofilm formation and antibiotic resistance in *Klebsiella pneumoniae* urinary strains. *J Appl Microbiol*, 123(4):1003-1018. https://doi.org/10.1111/jam.13533

Wang WD, Zhang NN, Chanda W, et al., 2018. Antibacterial and anti-biofilm activity of the lipid extract from *Mantidis ootheca* on *Pseudomonas aeruginosa*. *J Zhejiang Univ-Sci B (Biomed & Biotechnol)*, 19(5):364-371. https://doi.org/10.1631/jzus.B1700356

Wang XL, Zhu XC, Wang YS, et al., 2010. Isolation and identification of 8 strains of *Bacillus* and comparison of their resistance. *Vet Sci China*, 40(10):1017-1022 (in Chinese).

Whitchurch BC, Tolker-Nielsen T, Ragas PC, et al., 2002. Extracellular DNA required for bacterial biofilm formation. *Science*, 295(5559):1487. https://doi.org/10.1126/science.295.5559.1487

Yang D, Zhang Z, 2008. Biofilm-forming *Klebsiella pneumoniae* strains have greater likelihood of producing extended-spectrum β-lactamases. *J Hosp Infect*, 68(4): 369-371. https://doi.org/10.1016/j.jhin.2008.02.001

Yang F, Deng BG, Wei JD, et al., 2017. Drug-resistant and molecular characteristic of *Klebsiella pneumoniae* isolated from nosocomial and animal origins. *Chin J Zoonoses*, 33(10):888-892 (in Chinese). https://doi.org/10.3969/j.issn.1002-2694.2017.10.007

Yang QS, Meng XX, Xia L, et al., 2003. Conservation status and causes of decline of musk deer (*Moschus* spp.) in China. *Biol Conserv*, 109(3):333-342. https://doi.org/10.1016/s0006-3207(02)00159-3

Yao X, Feng L, Zhu GM, 2018. Molecular epidemiology and resistant mechanisms of carbapenem-resistant *Klebsiella pneumoniae*. *Chin J Antibiot*, 43(1):85-90 (in Chinese). https://doi.org/10.13461/j.cnki.cja.006161

Yuan JY, Xu XG, Hu FP, et al., 2018. Fluoroquinolone resistance profile of *Klebsiella pneumoniae* isolates and the mechanisms conferring antibiotic resistance in ST494 strains. *Chin J Infect Chemother*, 18(3):286-291 (in Chinese). https://doi.org/10.16718/j.1009-7708.2018.03.008

Zhai HL, Wang YF, 2017. Pathological changes of reactive thrombocytosis induced by recombinant human thrombopoietin in mice. *J Chongqing Med Univ*, 42(9):1161-1166 (in Chinese). https://doi.org/10.13406/j.cnki.cyxb.001018

Zhao W, Tian Q, Luo Y, et al., 2017a. Isolation, identification, and genome analysis of lung pathogenic *Klebsiella pneumoniae* (LPKP) in forest musk deer. *J Zoo Wildl Med*, 48(4):1039-1048. https://doi.org/10.1638/2016-0241.1

Zhao W, Wang WY, Cheng JG, et al., 2017b. Isolation and identification of *Klebsiella pneumoniae* from forest musk deer and bioinformatics analysis of its *kp05372* gene. *J Northwest A&F Univ (Nat Sci Ed)*, 45(12):23-30 (in Chinese). https://doi.org/10.13207/j.cnki.jnwafu.2017.12.004

Zhou XX, He TM, Peng GN, et al., 2013. Isolation, identification and resistance analysis of 7 *Bacillus* strains from the intestinal tract of giant panda. *Chin Vet Sci*, 43(11): 1115-1121 (in Chinese). https://doi.org/10.16656/j.issn.1673-4696.2013.11.011

Zhu H, Liu HJ, Ning SJ, et al., 2012. The response of type 2 quorum sensing in *Klebsiella pneumoniae* to a fluctuating culture environment. *DNA Cell Biol*, 31(4):455-459. https://doi.org/10.1089/dna.2011.1375

中文概要

题　目：LysR 家族新基因 *kp05372* 对林麝肺炎克雷伯氏菌的作用的初步研究

目　的：通过 *kp05372* 基因的敲除来研究其对林麝肺炎克雷伯氏菌生物表型的影响。

创新点：解析了 LysR 家族新基因 *kp05372* 对林麝肺炎克雷伯氏菌生物表型的影响。

方　法：通过基因敲除和回补技术构建了 *kp05372* 的基因缺失株和基因回补株，比较了 *kp05372* 基因缺失前后，林麝肺炎克雷伯氏菌在生长曲线、药敏试验、生物被膜、抗逆性、细菌半数致死量、定殖能力、病理形态学等生物学特性所表现出的差异。

结　论：成功构建了 *kp05372* 基因的缺失株及回补株。*kp05372* 基因的缺失导致林麝肺炎克雷伯氏菌耐药性和耐酸性发生了变化，毒力、生物膜和定殖能力降低，并且调控了上游临近区域的基因表达。

关键词：林麝；肺炎克雷伯氏菌；LysR 转录因子；*kp05372*；生物表型；上游基因